JOURNAL OF AIRCRAFT
Vol. 37, No. 4, July–August 2000

Testing of Semiactive Landing Gear Control for a General Aviation Aircraft

Gian Luca Ghiringhelli*
Politecnico di Milano, 20156 Milan, Italy

The operating possibilities of semiactive control of landing gears aimed at application to general aviation aircraft are evaluated. Compared to fully active systems, this kind of control is simple, lightweight, and safe, its intervention being based on the modification of the oil orifice section only. This active control was designed by using a landing simulation code that allowed a reliable prediction of its effectiveness. The application of the active shock absorber to a nonflying prototype has been both numerically and experimentally investigated, by means of drop tests at different sink speeds. The setup, the control strategy, and the obtained results are described, and the measured responses are compared to simulation results. Good agreement between analytical and experimental results confirms that a heuristic tuning of the active control can be effective when adequate simulation tools are used in the design.

Nomenclature

A = cross section or area
C = experimental flow coefficient
E = error in ground load
G = tire ground force
K = global coefficient relating viscous to elastic work $K(v_z, m, \ldots)$
k = control gains
L = lift force
m = system mass
p = initial pressure
R = outer tire radius
r = inner tire radius
S = forces produced by the shock absorber
T = kinetic energy related to the vertical motion
U = potential energy
V = initial volume
v = speed
W = work done by the subscript force
Z = vertical ground load
β = vertical displacement of the center of gravity
γ = polytropic exponent for compression law
δ = compression
η = landing gear efficiency
μ = shock-absorber friction coefficient in polynomial form $\mu(\delta_S)$
ν = friction coefficient for ground and tire
ρ = oil density

Subscripts

D = derivative gain
e = elastic (force produced by the shock absorber)
f = friction (force produced by the shock absorber)
G = gas
h = horizontal ground force
L = lift force parameter
M = measured vertical ground load
N = needed vertical ground load
O = optimal vertical ground load
o = oil
P = proportional gain
ref = reference paramater
S = shock-absorber parameters or properties
T = tire
t = total (force produced by the shock absorber)
v = related to viscous effects (force produced by the shock absorber)
X = orifice
z = vertical direction

Received 8 June 1999; revision received 4 December 1999; accepted for publication 8 December 1999.

*Associate Professor, Design of Aerospace Structures, Dipartimento di Ingegneria Aerospaziale, via La Masa 34; gianluca.ghiringhelli@polimi.it.

Introduction

FLIGHT regulations and competitive requirements demand performances that sometimes are conflicting with technical issues. For instance, a steep approach path and high vertical landing speeds would allow operation even in areas subject to noise restriction; the exploitation of semiprepared or scarcely maintained runways could enlarge the operating possibilities as well. However, these requirements conflict with the need to avoid high landing loads that could either reduce the fatigue life of several aircraft components or require more frequent inspections. Furthermore, it is known that fatigue is a key factor in a wide percentage of failures related to landing gears and their interface structure,[1,2] so that load reduction can result in a significant increase in the fatigue life of the related structural parts. A proper choice of materials and a careful design of details can reduce the influence of landing loads only up to a point; in fact, these loads are affected by several parameters that cannot be completely controlled. Landing gear is required to absorb energy in different operating conditions, that is, a wide range of parameters such as ground friction coefficient, aircraft overall weight, attitude, speed, etc., and a fixed parameter system can be completely satisfactory only in a limited number of cases. A metering pin improves performance by introducing a dependence of viscous dissipation on the shock-absorber motion. The natural evolution of this concept is a system with size parameters that are actively modified by means of an assigned dynamic criteria. Active control represents a possible answer to satisfying pressing and conflicting requirements in different operating conditions; landing gear design does not escape this philosophy.

Active control of landing gear is usually intended for the general improvement of the landing system efficiency and is aimed at broadening the operating limits, specifically, for the reduction of ground loads during touchdown and taxiing maneuvers. Other performance parameters can also be positively affected, particularly those related to the controllability of flexible aircraft, to the crew workload, and to the comfort of passengers. Both fully and semiactive control systems have been proposed and tested (see Fig. 1). The fully active approach has been extensively tested for military applications.[3–10]

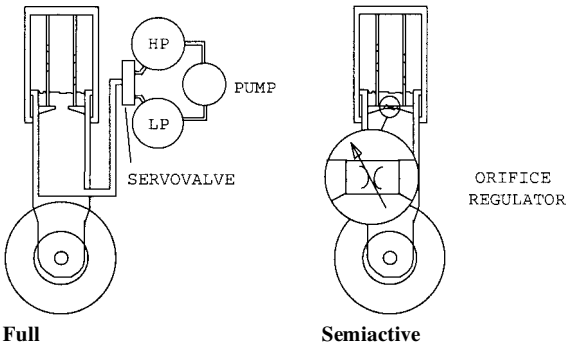

Fig. 1 Control devices.

It is based on the use of high- and low-pressure tanks, which allow putting/removing oil into/from the shock absorber and a pump that maintains the pressure into the tanks. This approach allows control of both the pneumatic and hydraulic terms of the damper force, but it can lead to complex systems and to a significant increase in weight, especially when safety and redundancy requirements are included. On the other hand, the good behavior when continuous disturbances are applied to the shock absorber, for example, loads due to a running over of either unprepared or repaired runways, makes this method very effective.

The semiactive approach is widely used in the automotive field,[11–13] but some aeronautical applications have been suggested and numerically evaluated.[6,14,15] In Ref. 14, a comparison with a fully active system is presented for landing impacts and runway disturbances, together with a study of both a failure detection scheme and a reliability assessment. The semiactive control approach is based on a variable metering-pin concept that is actively implemented to tailor the metering geometry to different operating conditions. Performances are not expected to be as good as those of a fully active control, but it is simpler, safer, and lighter, requiring only a device that controls the section of the orifice. Moreover, it does not introduce energy into the landing gear: In fact it simply works by controlling the amount of dissipation, and the control system shows a basic passive behavior with respect to the aircraft dynamics (both rigid and flexible) with no instability problems. The elastic energy that is stored in the gas chamber is released during the gear extension, and the system is always dissipative. Furthermore, low power is needed, and a retrofit can be quite simple, even if this is likely to require the substitution of the original shock absorber. Extensive preliminary numerical simulations confirmed that satisfactory results can be obtained with this active system. An internally developed simulation code [ground air and landing loads, (GRAALL[16,17])] has been modified to include the effects of the semiactive system under investigation.[15] The implementation of a deterministic controller behavior by means of a fuzzy logic correction has been also suggested, showing some significant improvement.[18] The same tool has been used to design the active control system presented here. The present work shows that real-time tuning of the orifice can be effective, even using low-performance driving devices, and that the active control strategy, based on a heuristic definition of control parameter maps, can be designed using simulation tools. The semiactive control strategy has been applied to the oleo-pneumatic shock absorber of the main gear of a light aircraft; a nonflying shock absorber, controlled by a personal computer, has been built, and the active control effectiveness has been investigated by performing several drop tests.

Active Control Strategy

The ideal landing gear is characterized by elastic–plastic behavior in terms of vertical loads induced at touchdown: The force should rise as fast as possible to the maximum allowed value, then remain constant until the maximum c.g. stroke is reached, and decay afterward. An initial steep gradient of the vertical load is desirable, to allow a gradual spinup of the wheel; in this way the vertical force will not rise to excessive values when high friction coefficients are present. Otherwise springback phenomena would be exacerbated by the corresponding horizontal loads.

In this work the active control strategy has been envisaged to attempt the optimization of the efficiency of the landing gear accounting for this physical interpretation of the phenomenon. The efficiency of the landing gear system is defined in the usual form,

$$\eta = \frac{\int_0^{\beta_{\max}} Z \, \mathrm{d}\beta}{\beta_{\max} Z_{\max}} \tag{1}$$

According to the semiactive control policy, the controller regulates the section of the orifice of the damper to obtain the optimal behavior of the landing gear. To achieve the best advantage from the use of the active control, the target load is made dependent on the specific maneuver. A preliminary procedure has been introduced to predict a case-dependent maximum load: The situation is energetically analyzed to minimize vertical ground loads by fully exploiting the shock-absorber capabilities. The advantages to several aspects of the structural problems, in particular the fatigue life, are evident.

The procedure to be described worked well in the case of drop tests; however, simple adjustments have been identified and successfully tested by simulating both symmetric and unsymmetric landings of a complete aircraft equipped with actively controlled main gears.

Preliminary Step to Estimate Maximum Vertical Loads

To define the optimal profile of the ground vertical load, energy balance is used taking into account the kinetic energy associated with the vertical motion, the potential energy, and the work done by the lift force. As a first approximation, the tire internal work is assumed to be included into the shock-absorber one, then the work done by external forces can be equated to the work done by the shock absorber in the energy balance equation:

$$\Delta T + \Delta U + W_L \approx W_S \tag{2}$$

In Eq. (2) ΔT is the change in the kinetic energy, ΔU is the change in the potential energy, W_L is the work of lift forces, and W_S is the internal work of the shock absorber.

The left-hand side of Eq. (2) can be easily approximated. The horizontal component of the speed is assumed to remain constant during the initial phase of the touchdown, so that the change in kinetic energy is simply given by $\Delta T \approx \frac{1}{2} m v_z^2$. This term is known, provided that a measure of the vertical speed and an estimate of the landing mass are available. The other terms on the left-hand side can be roughly approximated once an estimate of the center of gravity vertical displacement is available; as an example, it can be predicted by means of the landing gear efficiency. The work done by the lift forces is unknown, and it is often approximated by a fraction, for example, $\frac{2}{3}$, of the change in potential energy; the availability of the c.g. vertical displacement also contributes this term.

The change in the potential energy is often neglected when the writing of Eq. (2) is aimed at finding maximum landing loads. Indeed this approximation does not affect results at high sink speed, but it becomes influential when the sink speed decreases; thus, it has been accounted for to allow a better evaluation of the maneuver. To approximate this term, a tuning map has been preferred to the use of the prediction of the landing gear efficiency previously envisaged. It supplies the c.g. displacement as function of maneuver parameters, for example, sink speed, mass, attitude, that is, $\beta = f(V_z, m, \ldots)$.

The exploitation of the energy balance equation to obtain the maximum ground loads requires writing the right-hand side of Eq. (2) in terms of maximum shock-absorber load and stroke. We failed in writing a separate estimate of the elastic and viscous contributions to the work, and so a global formulation was envisaged by using the following equation:

$$W_S \approx K \int_0^{\delta_S} S_E \, \mathrm{d}\delta \tag{3}$$

where S_E is the elastic contribution to the shock-absorber internal force. It entails having a suitable model of the elastic force and a

single coefficient K (function of several maneuver parameters, e.g., sink speed, mass, attitude, etc.) that allows the analytical evaluation of the work done by the shock absorber based on the knowledge of the elastic force behavior alone. The assumption is supported by the idea that this coefficient can be conveniently mapped in advance, with respect to maneuver parameters, by extensively exploiting the simulations, once a validated model of the landing gear is available. In the present work, a low-order polynomial depending on the sink speed only has been assumed. The elastic force can be easily modeled by the well-known polytropic approximation that yields an analytical form of the force due to the gas chamber compression, that is, S_e, as a function of the shock-absorber stroke δ_S [Eq. (8) in the Shock-Absorber Model section]. Equation (3) is solved, simultaneously obtaining the maximum values of shock-absorber stroke and force; the ground load corresponding to the latter is assumed to define the optimal profile of ground loads during the touchdown. It is shaped to allow a gradual spinup of the wheel, needed to avoid excessive friction forces between tire and ground. In Fig. 2, the forces are defined. In Fig. 3, a flow chart of the procedure is presented. The use of this procedure leads to results that include both the actual properties of the shock-absorber and the landing conditions. The sensitivity of this equation to the errors in the mass estimates has been presented in Ref. 15, showing satisfactory robustness of the approach.

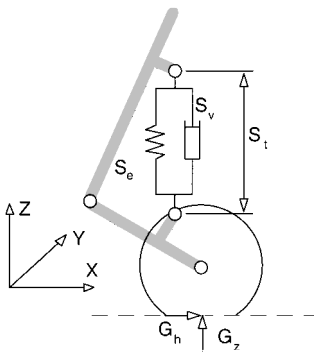

Fig. 2 Forces definition.

Active Control

The controller operations are now described, in relation to the flow chart presented in Fig. 4. Starting from touchdown, the controller tries to follow the optimal load profile designed in the preliminary phase. In previous works,[15,18] a strategy based on three inputs (vertical speed, shock-absorber stroke, and stroke time rate) has been used. It is first described here. To control effectively the damping by regulating the viscous force only, the shock-absorber internal load S_t is needed. It is computed from the optimal ground force Z_O by means of appropriate transformations, depending on the landing gear geometry:

$$S_t = f(Z_O) \tag{4}$$

The actual presence of the horizontal ground force can be accounted for by means of a triangular pulse scheme that represents a good approximation of the actual behavior; this approach is quite rough but it is justified by the short duration of the horizontal force, which quickly decays as the wheel spins up. Moreover, in previous work,[15] it has been completely neglected, nonetheless obtaining satisfactory results.

The semiactive control exploits its intervention on the viscous force only. The controller can determine the viscous force needed to follow an optimal profile with the simple equation

$$S_v = S_t - S_e \tag{5}$$

by assuming the availability of an estimate of the elastic portion of the shock-absorber force S_e; the polytropic model described in the Shock-Absorber Model section [Eq. (8)] is used for this purpose. The value of the orifice cross section, required to obtain the desired drop pressure, is obtained by solving the equation for the viscous force of the shock absorber, that is, Eq. (9), with respect to this parameter.

To match the actual operating conditions better, the control system modifies the target by means of a proportional and derivative correction. An estimate of the actual vertical ground load Z_M, obtained through the measure of the vertical acceleration and an estimate of the reduced mass, supplies a compensation term, proportional to the difference between the optimal and the actual vertical load, that is, the error $E = Z_O - Z_M$, as well as a derivative compensation term

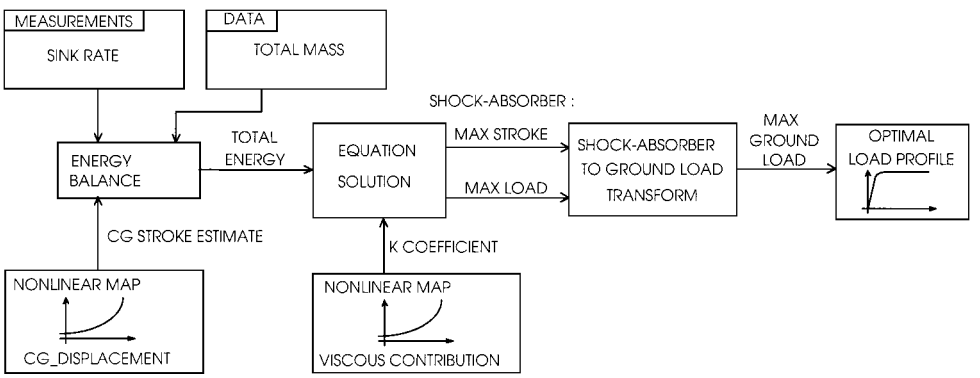

Fig. 3 Preliminary procedure flow chart.

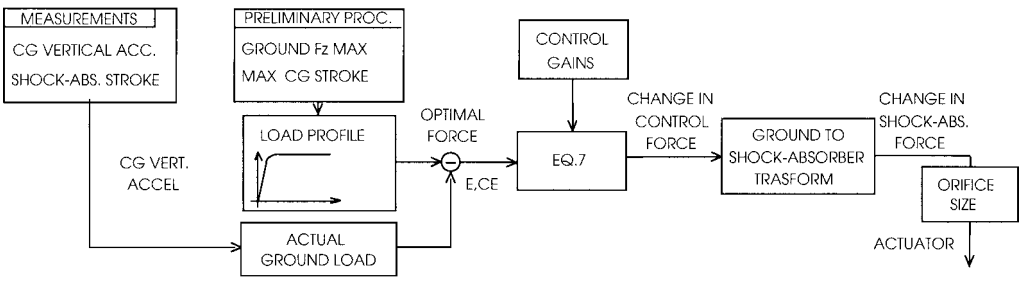

Fig. 4 Active control flow chart.

related to the time rate of the error, that is, $\dot{E}$. This simple correction became very useful in achieving optimal performances. Then the following equation of the desired ground load is obtained:

$$Z_N = Z_O + Ek_P + \dot{E}k_D \tag{6}$$

which is used to compute the shock-absorber load by means of Eq. (4).

As reported in Refs. 15 and 18, this law works well but requires a suitable model of both the viscous dissipation and the gas stiffness. Therefore, a simpler strategy, not requiring the shock-absorber stroke measurement, has been envisaged. Because the load change is entirely realized by the change in the oil orifice cross section, the change in total force alone can be used to obtain the change in the orifice cross section. Then in Eq. (4), the following incremental term in the needed ground load replaces the total one:

$$\Delta Z_N = Ek_P + \dot{E}k_P \tag{7}$$

Once transformed into the corresponding shock-absorber load change, the equation supplying the viscous pressure drop again can be used to determine the control action in terms of change in orifice cross section. With this approach, only two measurements, that is, shock-absorber speed and vertical ground load, are needed. The gains in Eqs. (6) and (7), k_P and k_D, are evaluated by a trial and error procedure based on numerical simulations.

Finally, the current input, required to obtain the desired pressure drop, is evaluated and used to drive the servovalve, accounting for possible saturation of the actuation device. A dynamic compensation could be included to improve the servovalve response, but there has been no need for this yet.

The control is triggered by an accelerometer located on the oscillating brace; it can be also used to control landing loads during rollout on a rough runway.

Maps Setting

The proposed semiactive approach requires the preparation of two maps. In this section the procedures adopted for this task are described.

The first map supplies the vertical displacement of the center of gravity with respect to maneuver parameters. It is evaluated by fitting data obtained analytically by simulating drop tests with a model of the passive shock absorber. This map supplies an approximate evaluation of the change in potential energy that is rough but precise enough to catch the essence of the phenomenon. Alternatively, an estimate of the landing gear efficiency could be used to obtain this result; however, this parameter implicitly depends on the landing gear behavior, thus preventing the explicitness of the shock-absorber parameters. Therefore, the use of a function that maps the vertical displacement of the center of gravity has been preferred.

The global coefficient K must be supplied to solve Eq. (3), with respect to maximum shock-absorber load and stroke, allowing one to account for the effectiveness of active control in several landing conditions. This task is exploited by using a map, for example, $K = K(v_z, m)$, built by points: Each point is determined by a trial and error procedure that allows one to define the values of the parameter K by maximizing the landing gear performances for several maneuver parameters, for example, for different sink speeds and masses. Each evaluation requires a tuning exploited by means of the comparison of ground load time history, provided by the simulations performed with the active shock absorber, and the optimal load profile, obtained for an assigned K. The optimal load must be intuitively addressed to correct values by changing K. Too high expected loads determine the closure of the orifice, leading to a very stiff landing, small center of gravity displacement, and shock-absorber stroke; in this case, the energy associated to viscous forces is prevalent in the energy balance. Furthermore, even if efficiency can be high, loads can become excessive for the maneuver at hand. However, excessively low expected loads would lead to a reduced viscous dissipation because the controller would keep the orifice open, so that large shock-absorber strokes would be needed to absorb the landing energy. This entails high elastic reactions at the end of the compression and basically low efficiency. In this job one can be helped by the following observation: Values of K higher/lower than needed entail lower/higher optimal load.

This procedure is carried out with a simple proportional correction in Eq. (7), that is $k_P = 1$ and $k_D = 0$; then a performance improvement can be achieved by tuning the gains.

The test at hand is a simplified case; therefore, due to constant drop mass and attitude, two simple tables are supplied and a quadratic interpolation in a single variable is determined by a least-square fit in terms of the sink speed.

Obviously the presence of the active control redefines these maps. They should be evaluated again by iterating the procedure. Indeed the process has been stopped after the first step. In all of the tested cases, satisfactory results have been obtained with maps at the first step, and further iterations did not significantly improve the control performances.

Drop Test Simulation

It is possible to design the active control analytically by hand by solving the described equations and defining the coefficient for the evaluation of the internal work of the shock absorber with a few trials. The availability of a reliable code for landing and drop test simulations led to a more accurate numerical development of the tuning procedure. Indeed, the drop test dynamic model is very simple. It is based on a kinematic description of the gear, with the structural flexibility neglected, so that only three degrees of freedom are actually integrated: the vertical position, the slope angle of the oscillating brace, and the wheel rotation. Here only the models of the two elements directly involved in the problem at hand are presented; they are the shock-absorber and the tire models, both described in a simplified mode. In Refs. 16 and 17, the reader will find an exhaustive discussion of the general capabilities of the code, which, first modified in Ref. 15, has been upgraded to account for a discrete active control and for dynamic properties of the servovalve. The transfer function of this device has been implemented as a second-order model.

Shock-Absorber Model

The shock absorber is modeled as a line force element that introduces into the structure a load depending on the relative position and velocity of its ends. The stiffness and damping properties of an oleo-pneumatic shock absorber can be conveniently represented by explicit forces related to both the energy stored into the gas chamber and the energy dissipated by the oil flow through the orifice. Thus, two independent terms can be evaluated and then summed. This model has been well known for many years, for example, see Refs. 7 and 19, and is only briefly recalled here for sake of completeness. A polytropic model can be conveniently applied, so that the force is related to the initial precharge pressure p_G and to the ratio between initial and actual chamber volumes through the polytropic exponent γ_G. The elastic force can be evaluated by the following equation:

$$S_e = p_G A_G [V_G/(V_G - \Delta V_G)]^{\gamma_G} \tag{8}$$

where A_G is the gas chamber cross section and V_G and ΔV_G are the initial volume and its change, respectively.

As far as the viscous term is concerned, a model based on the evaluation of the inertia forces acting on the oil, when accelerated through the orifice by the shock-absorber motion, leads to the following equation:

$$S_v = \frac{1}{2}\rho \frac{A_O^3 v_S |v_S|}{A_X^2 C^2} \tag{9}$$

In this equation, A_O and A_X are the area of the oil piston and of the orifice, respectively, v_S is the shock-absorber speed, and C is an experimental flow coefficient, depending on a number of parameters, for example, Reynolds number, orifice geometry, and oil temperature.

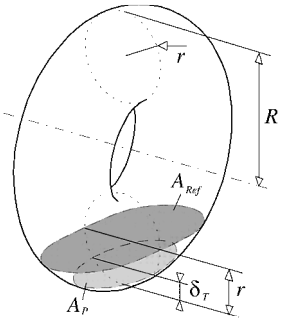

Fig. 5 Tire toroidal model.

Hysteretical phenomena due to the kinetic friction can be accounted for by means of a term proportional to the elastic force in the following way:

$$S_f = S_e \mu(\delta_S) \tanh(\dot{\delta}_S / v_{\text{ref}}) \tag{10}$$

where $\mu(\delta_S)$ is a polynomial form of the friction coefficient, depending on the shock-absorber stroke. The hyperbolic tangent is used, instead of the sign of the velocity $\dot{\delta}_S$, to avoid sudden changes in the sign of the friction force when the shock-absorber speed approaches zero, thus preventing possible numerical problems.

Tire Model

The tire is described as a rigid body, having toroidal shape, that interacts with a rigid flat ground by exchanging forces that depend on the volume of the geometric intersection. A variety of tire models can be found in the literature, suitable for several kinds of analyses.[20–26] However, in the cases characterized by a negligible contribution of the tire dynamics, for example, the touchdown, a simplified model is recommended. Tires commonly used in aircraft can be geometrically modeled as toruses (see Fig. 5); this allows building a model that requires very few basic parameters, such as the external radius, the section radius, the internal pressure, and a volume coefficient needed to account for the actual internal volume of the tire. The tire contribution to the landing dynamics can be conveniently described by means of a simple polytropic law, relating changes in the inflating pressure to changes in the internal volume, and the actual footprint area, leading to the following equation of the vertical ground load:

$$G_z = A_T p_T \left(\frac{V_T}{V_T - \Delta V_T} \right)^{\gamma_T} \left[1 + \tanh\left(\frac{\dot{\delta}_T}{v_{\text{ref}}} \right) \right] \tag{11}$$

The torus volume V_T is evaluated by means of the geometric terms, the outer and inner radii R and r, and of a volume coefficient that reduces the nominal volume to the effective internal one, accounting for several parameters (tire thickness and shape, wheel profile, etc.). The change in volume ΔV_T is computed by intersecting the ground with the tire. This task is not trivial, and it has been simplified by assuming the ground as a rigid wall; then the following approximation of the contact volume is obtained:

$$\Delta V_T = \tfrac{1}{2} A_T \delta_T \tag{12}$$

This, in turn, is evaluated by linearly scaling a reference area A_{ref} resulting from the intersection of an horizontal plane, placed at the middle of the torus, with the torus itself (as shown in Fig. 5), that is,

$$A_T = A_{\text{ref}} \delta_T / r \tag{13}$$

The reference area is approximated as an ellipse, whose semiaxes are given by r and $\sqrt{[R^2 - (R - r)^2]}$, respectively. The evaluation of the footprint area depends only on the geometric sizes and the actual tire deflection, irrespective of the actual tire lateral attitude and deformation.

In Eq. (11) an hyperbolic term is introduced to account for tire internal dissipation; it depends on the compression speed $\dot{\delta}_T$ and a reference speed v_{ref}.

The horizontal forces can be evaluated by means of the following equation:

$$G_h = \nu_T \nu_G G_z \tanh(v_h / v_{\text{ref}}) \tag{14}$$

Appropriate kinetic friction coefficients ν_T and ν_G have been introduced. The one related to the tire depends on the peripheral relative speed v_h at the footprint centroid, by means of related slip ratios: This accounts for the possible presence of a transversal sliding. In this case, G_h must be projected to evaluate forces and moments acting on the wheel axle. Despite its simplicity, this model is suitable for aircraft tire problems where the transversal deformation is small during conventional touchdowns. To simulate conveniently other phenomena, for example, shimmy, one of the aforementioned more sophisticated models is needed.

Experimental Setup Description

A description of the experimental setup is provided, along with basic data for the landing gear.

Drop Test Facility

The drop test facility is a vertical test fixture, made of two vertical steel rails that guide a sliding carriage (see Fig. 6). The maximum drop height is 5 m, well above the value required for usual tests on aircraft landing gears. Lift has not been reproduced during the present tests. The following measurements are collected by the data acquisition system: center of gravity position and acceleration, measured using a digital encoder and a piezoresistive accelerometer; shock-absorber stroke, provided by a linear potentiometer; two piezoresistive accelerometers located at the ends of the shock absorber to estimate the shock-absorber speed; and pressure drop across the servovalve as supplied by a differential pressure measurement. Only some of them are used by the active control system. The output of a photocell is used to start the acquisition, whereas an accelerometer signal is used to trigger the control.

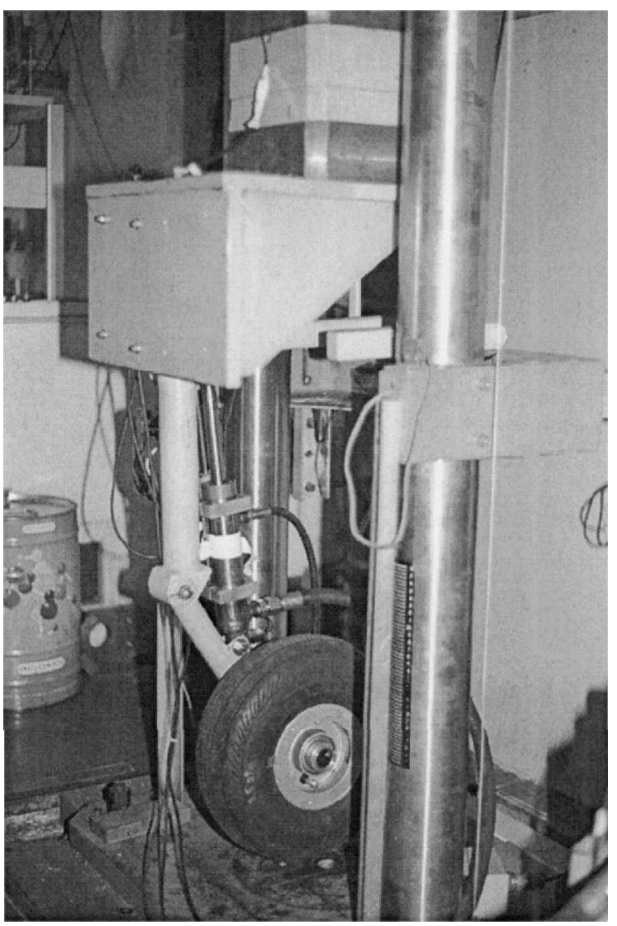

Fig. 6 Landing gear with the modified shock absorber.

Landing Gear Description

The main carriage of a light jet trainer has been used in the present activity. It is an articulated landing gear equipped with a standard oleo-pneumatic shock absorber (Fig. 6); its main properties are summarized in Table 1. The drop ballast mass, based on applicable aviation regulations, has been computed as 275 kg.

The standard shock absorber of this landing gear is an oleo strut with no floating piston to separate the oil from the pressured gas; nitrogen is used to precharge the gas chamber. To simplify the realization of the active control experiment, this device has been replaced by a single acting jack connected to an external hydraulic circuit that restores the elastic and viscous effects of the original shock absorber, thanks to the presence of a controlled servovalve that regulates the oil orifice and a high-pressure accumulator. The system is shown in Fig. 7, where the independent hydraulic system needed to drive the servovalve is shown. The latter is a standard commercial device (MOOG Model D760 driven by a current input) whose main properties are summarized in Table 2. The selection of this valve was supported by an analysis of the frequency spectrum of the control input of an ideal device,[15] which indicated that above 40 Hz the energy content was negligible. On the other hand, this kind of system is suitable for low-cost experimental investigation of the semiactive control system. The main internal dimensions of the original shock absorber have been maintained for the new device, so that the performance changes of the landing gear are negligible, as will be show in the following.

Table 1 Landing gear data

Property	Value
Drop ballast mass, kg	275
Gas pressure, MPa	3.53
Gas chamber diameter, mm	36
Gas chamber initial length, mm	177
Oil piston diameter, mm	36
Maximum stroke, mm	125
Oil orifice diameter (compression), mm	2
Oil orifice diameter (extension), mm	1.75
Shock-absorber length, mm	440
Tire pressure, MPa	0.35
Tire external diameter, mm	340
Tire torus diameter, mm	110

Table 2 Servovalve properties

Property	Value
Working pressure	210 bar
Nominal flow	65 l/min ± 10%
Driving type	External
Frequency response	40 Hz
Damping	0.5%
Nominal current (maximum flow)	40 mA

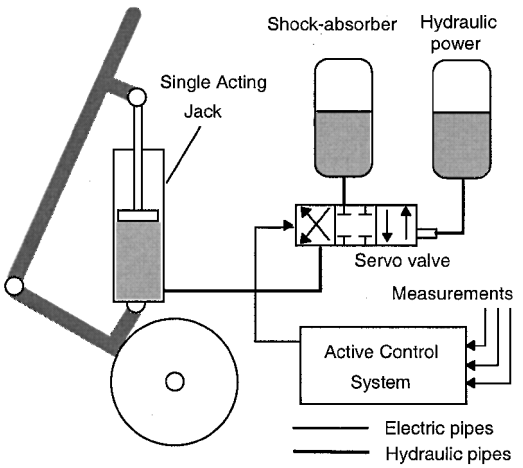

Fig. 7 Hydraulic equivalent plant.

Digital Control

The shock absorber is driven by a digital controller implemented in a computer code running on a 486 25-MHz personal computer in real-time mode. To implement the described control strategy, the computer has been equipped with an Intelligent Instrumentation board that provides eight multiplexed 12-bit A/D channels (the A/D converter maximum rate is 100 kHz) and two 12-bit D/A channels. The maximum active control frequency allowed by this system is 2.0 kHz. The servovalve is always actuated by the computer: It works as an intelligent oil orifice, in the active mode, when a time-variable input is supplied; the hydraulic plant behaves as a standard shock absorber when a fixed current is applied, that is, it operates as a passive device. The output can be evaluated by the controller in terms of either orifice cross section or drop pressure. Actually the servovalve at hand is driven by a current input; this one is established on the basis of manufacturer data sheet, to obtain the desired drop pressure.

Preliminary Activities

As already mentioned, the landing gear shock absorber has been modified, by using an external hydraulic circuit, to simplify the implementation of the active control. Because the main dimensions have been maintained, a good correspondence between the performance of the modified landing gear and of the original one has been obtained, as demonstrated by the comparison of vertical acceleration time histories shown in Fig. 8. A drop test with no running wheel is used as reference, the sink speed (2.6 m/s) being defined by applicable aviation regulations. Results shown here refer to both experimental measurements and numerical results of the original and the modified shock absorbers. The correct posttouchdown response, that is, the agreement of simulated and measured responses after 0.8 s, has been actually achieved only when the change in oil viscous properties, due to the change in temperature during touchdown, was accounted for. As already mentioned, the passive behavior of the modified shock absorber has been obtained by using a

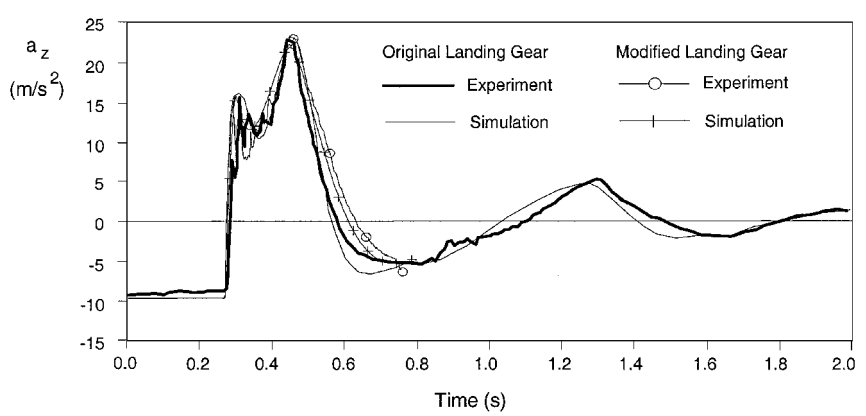

Fig. 8 Vertical acceleration time histories.

constant control input, that is, a fixed orifice size. A more exhaustive comparison between simulation results and experimental measurements is needed to support the design of the semiactive shock absorber. In Figs. 9 and 10, simulated and measured responses are compared at three sinking speeds (1.5, 2.0, and 2.5 m/s). All of them show satisfactory agreement. In Fig. 9, the vertical acceleration of the drop mass is presented, whereas in Fig. 10, the efficiency diagrams of the landing gear are shown. Finally, the comparison of both the shock-absorber stroke and the internal pressure is presented in Figs. 11 and 12.

The system behavior is correctly predicted by the simulations, but oscillations, related to the flexibility of both the landing gear and the drop test facility itself, are present.

Semi-Active Control Performances

Because a satisfactory model of the passive landing gear is available, the design of the active control and its performance evaluation have been carried out by means of the simulation code. In this section, the achievable performances are described, and the behavior of significant parameters is presented, along with a comparative analysis related to different passive designs.

In the case at hand, the tuning of the map needed by the control to contribute the optimal ground load led to an almost constant behavior of K with respect to the sink speed. The control

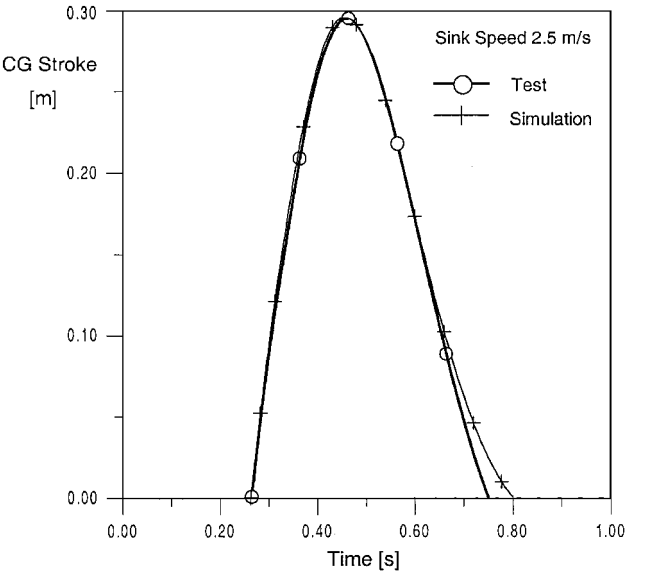

Fig. 11 Comparison between experimental and numerical c.g. displacement.

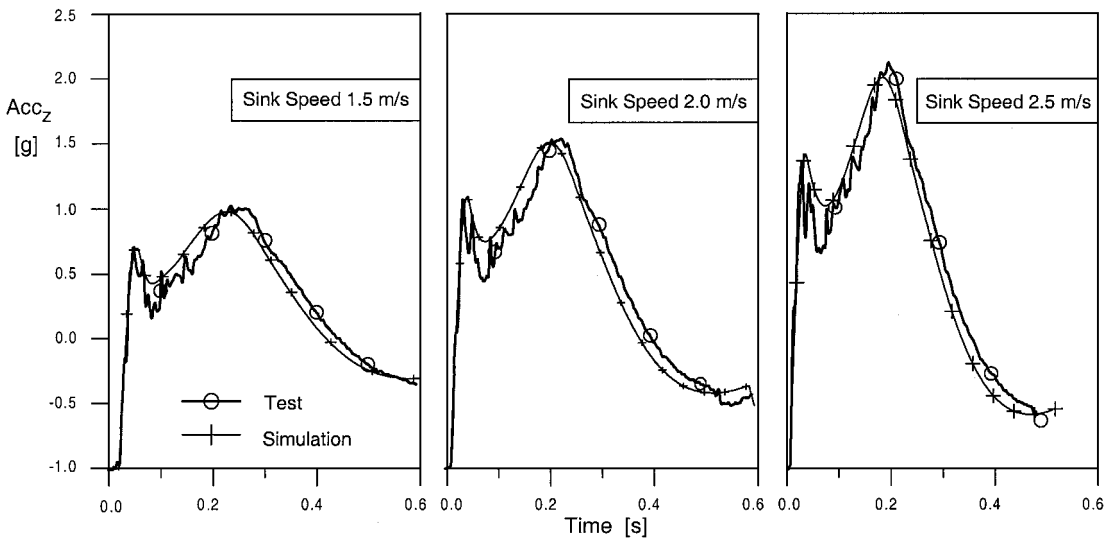

Fig. 9 Comparison between experimental and numerical c.g. acceleration.

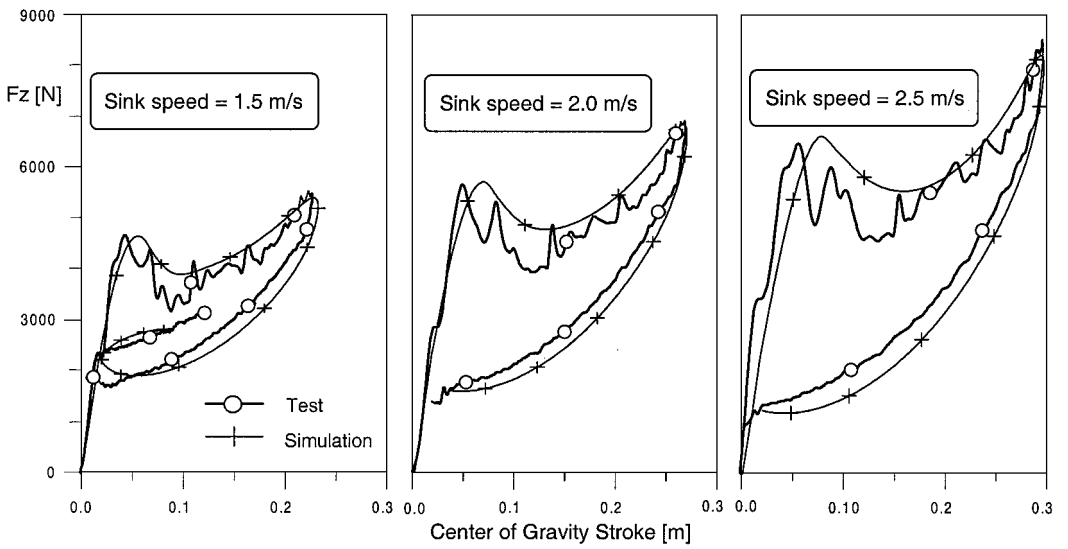

Fig. 10 Comparison between experimental and numerical efficiency diagrams.

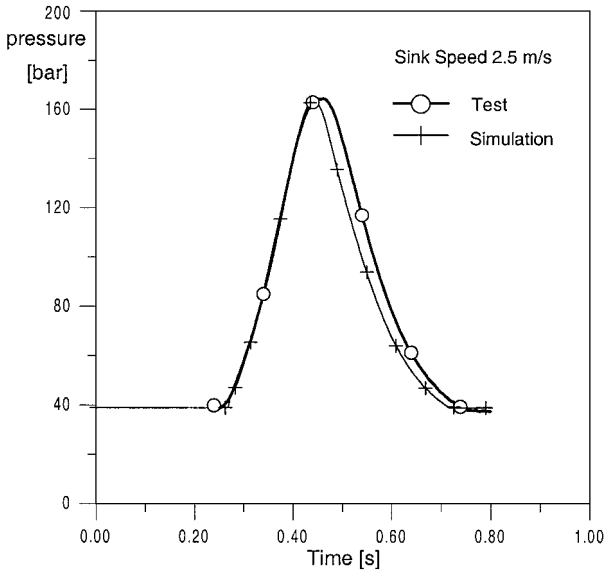

Fig. 12 Comparison between experimental and numerical shock-absorber internal pressure.

parameters tuned by means of the simulations required only slight adjustments during the experimental investigation. The predicted optimal ground loads for planned drop tests are summarized in Table 3. The control algorithm needs two gains to be defined, that is, proportional and derivative gains with respect to the error in ground load. Even if a systematic gain design is possible, a trial and error procedure has been preferred for the preliminary phase. This approach has been maintained because good results were promptly and easily obtained. The procedure led to the determination of values summarized in Table 3. Note that constant gains have been scheduled irrespective of sink speeds: actually they have been adjusted at the maximum sink speed and then are also used for lower values.

In Figs. 13 and 14, the time histories of the vertical acceleration and the efficiency diagrams of the landing gear are presented for the three reference sink speeds. Selected sink rates ranged from a minimum value to nearly the maximum indicated by the regulations for

Table 3 Semiactive control parameters

Sink speed, m/s	k_P	k_D	L, N
1.5	1.8	24	5056
2.0	1.8	24	6074
2.5	1.8	24	7122

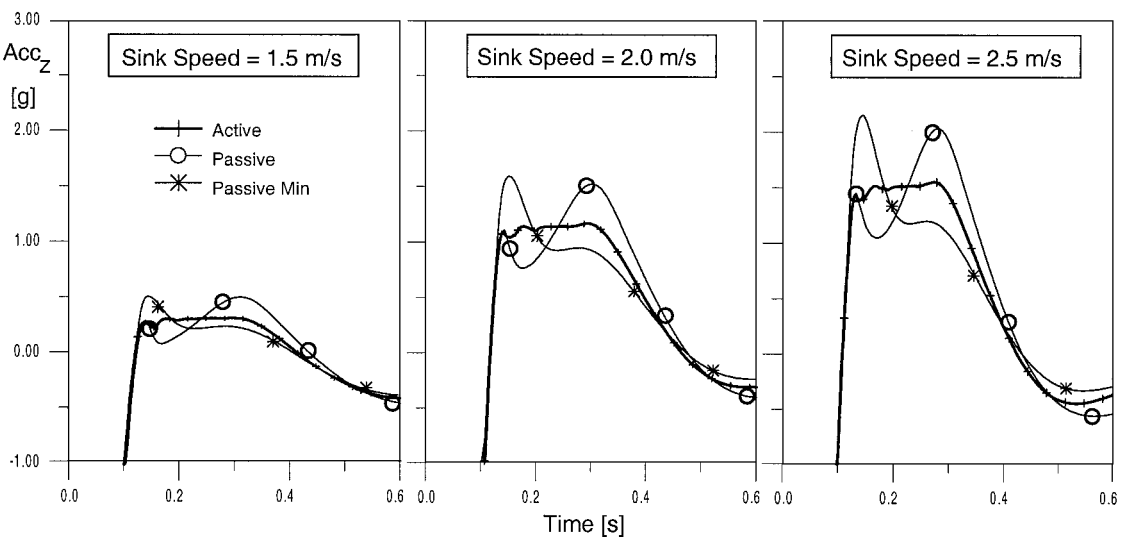

Fig. 13 Active control effectiveness.

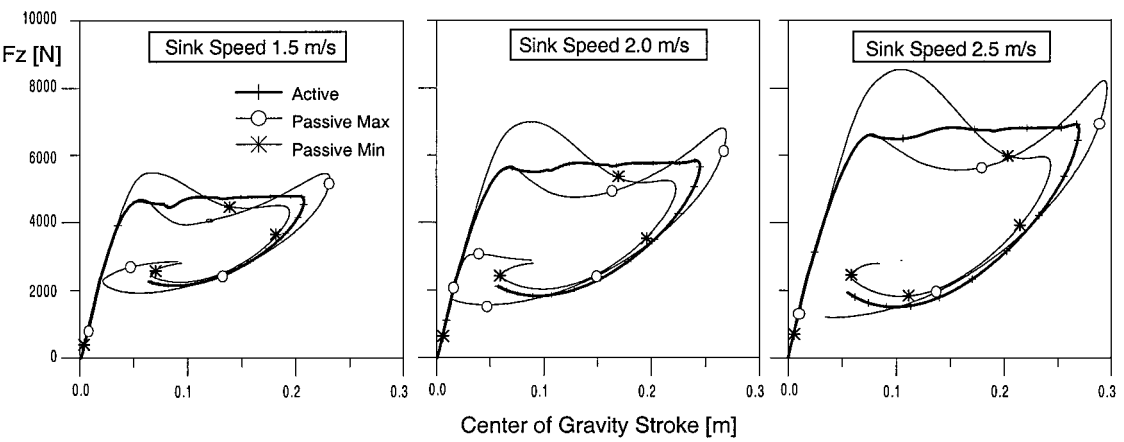

Fig. 14 Active control efficiency diagrams.

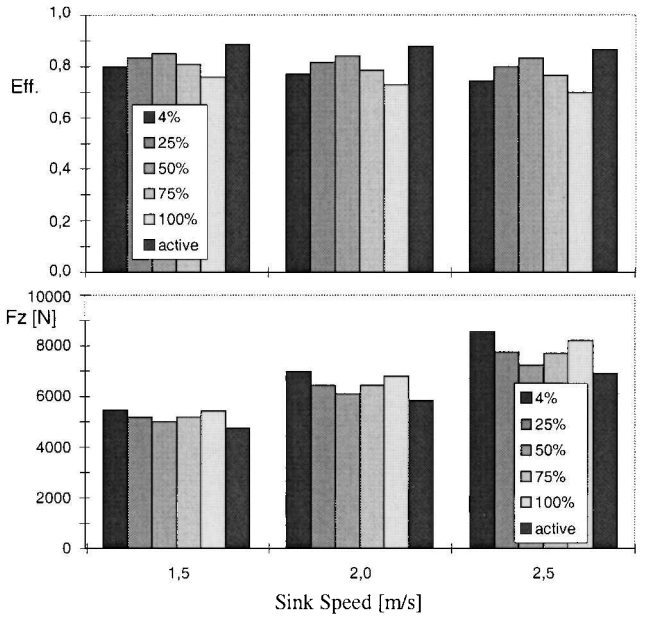

Fig. 15 Landing gear efficiencies and ground loads (numerical) as a function of the orifice size.

an aircraft of that category. Figures 13 and 14 clearly show the performance improvement: The load factor related to the maneuver is reduced regardless of the sink speed, and the efficiency of the landing gear is generally enhanced; a 15% load reduction is provided by the active control, as well as a similar improvement in the landing gear efficiency. The behavior of the original shock absorber was obtained by driving the servovalve with the maximum current input, that is, at the maximum orifice size. Data related to a shock absorber characterized by higher dissipation properties, that is, smaller orifice, are supplied in Figs. 13 and 14 as a further comparison. In Figs. 13 and 14, they appear with Passive Min label, showing a pronounced load peak at the beginning of the touchdown, due to the presence of relevant viscous effects. Figures 13 and 14 show that the active control increases the efficiency of the landing gear and that the reduction of both the center of gravity displacement and the ground vertical load is achieved. The behavior of the landing gear is optimized by the active control with respect to situations where either the elastic or the viscous shock-absorber response prevails. The shock absorber characterized by a higher dissipation reduces the center of gravity displacement, too, but the efficiency is not improved, resulting in an increase of the vertical loads.

Simulations have been also carried out to evaluate the effectiveness of an optimized passive design, using different oil orifice sections, ranging from a very small one to the maximum value by varying the servovalve current input from 4 to 100%. The results are shown by the bar charts presented in Figs. 15, where the efficiency

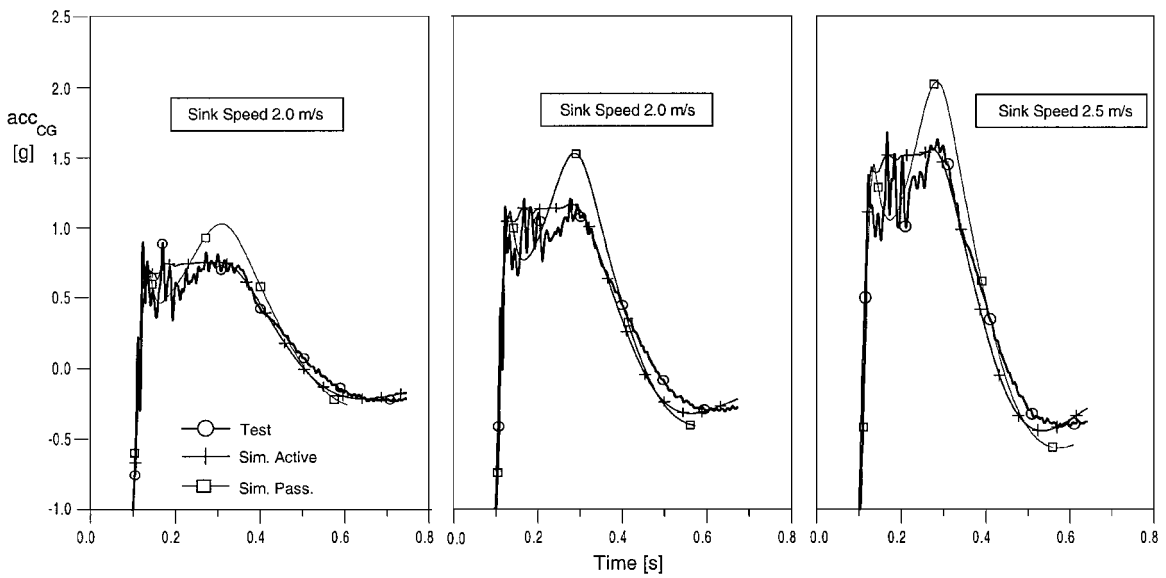

Fig. 16 Vertical acceleration: active test vs active and passive simulations.

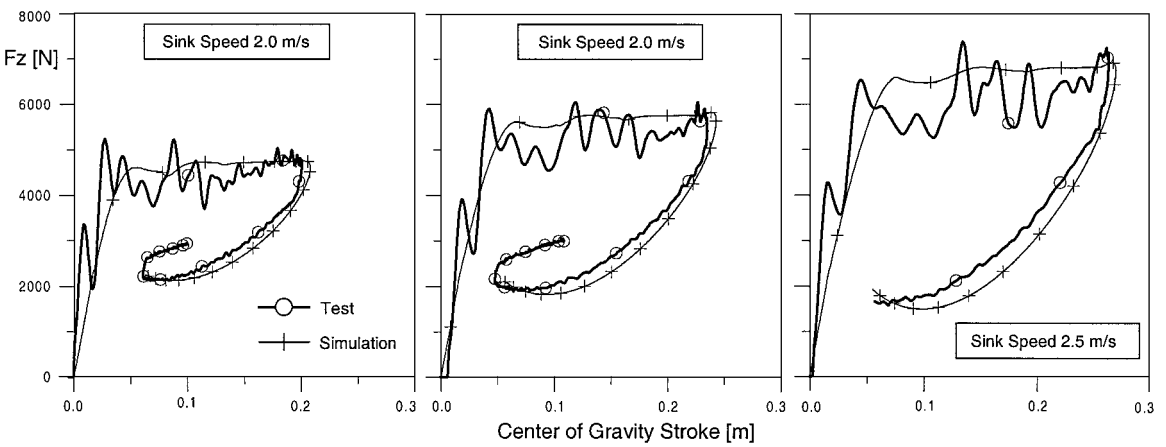

Fig. 17 Efficiency diagrams in the active case: test vs simulations.

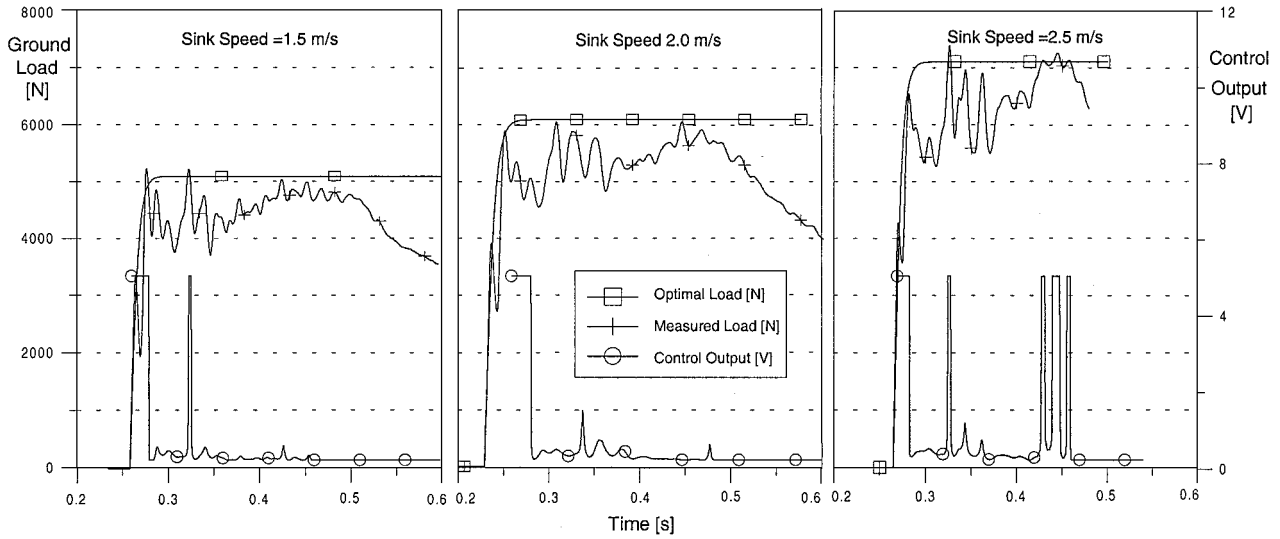

Fig. 18 Active control parameters time histories.

and vertical load in different conditions are compared. The active shock absorber provided the best performance even if an accurate passive design, that is, with an appropriate oil orifice area, leads to well-behaved responses for the problem at hand. Indeed, a change in mass or landing attitude could modify this situation.

Active Control Testing

Following the indications supplied by the simulations, the experimental setup has been adjusted. The digital control frequency used during this set of tests is 2000 Hz. A 500-Hz low-pass antialiasing filter has been used. The controller also exploits a digital filter, whose corner frequency is 100 Hz, to cancel structural vibrations from the measurements. In Figs. 16, the time histories of the vertical acceleration of the center of gravity are again shown at three sink speeds. A comparison between experimental measurements and simulation results related to both passive and semiactive modes is presented; in Figs. 16, the experimental time histories related to the passive mode are not shown for sake of clarity. In Figs. 17, the gear efficiency diagrams, based on simulated and measured responses, are again shown at three sink speeds in the active case. The examination of the experimental results confirms the predictions in load reduction supplied by the simulations. Experimental and simulated time histories are similar even if differences are more evident than in the passive case. Figures 18 show the behavior of the control output in relation to both actual and optimal ground loads. It is evident how the control activity heavily depends on the operating conditions. The comparative evaluation of the curves shows that a smoother behavior is recommendable and that, in some cases, the control intervention seems to be not fast enough. High-frequency oscillations are present in the experimental responses, showing a rougher behavior than in the passive case. This is explained by taking into account that the active control operates on measurements affected by structural vibrations that are only partially filtered: A more effective filtering can be exploited once negligible errors in phase will be ensured.

Conclusions

The work confirmed the effectiveness of a semiactive control of the shock absorber in the reduction of ground loads at landing. A nonflying prototype of the active shock absorber of a general aviation aircraft, implemented using a standard commercial electrohydraulic device, has been successfully tested. The controller has been designed by numerically simulating drop tests carried out with simple passive/active models, and a good agreement between numerical predictions and experimental measurements has been obtained in a range of sink speeds. The adopted controller strategy is based on a physical interpretation of the phenomenon; this allowed an easy tuning of the parameters, supported by comprehensive simulations. The results presented confirm the soundness of the adopted simulation tool and, in general, the effectiveness of the numerical simulation in the dynamic analysis of complex systems. Based on the availability of suitable and certified models, further investigation can be widely supported by simulation, thus reducing the need for expensive and time consuming experimental activities. The semiactive control allows cheaper and simpler devices compared to a fully active system, and so as soon as suitable devices become available, it will be a viable design choice. The retrofit of operating landing gears is possible without major modification, even on light aircrafts.

Acknowledgments

The author wishes to acknowledge the contributions of P. Carbognin and A. Perego to the experimental activities.

References

[1]Beaudet, P., and Roth, M., "Failure Analysis Case Histories of Canadian Forces Aircraft Landing Gear Components," *Landing Gear Design Loads Conference*, CP-484, AGARD, No. 1, 1991, pp. 1.1–1.24.

[2]Ladda, V., "Operational Loads on Landing Gear," *Landing Gear Design Loads Conference*, CP-484, AGARD, No. 11, 1991, pp. 11.1–11.16.

[3]Bender, E. K., and Beiber, M., "A Feasibility Study of Active Landing Gear," U.S. Air Force Flight Dynamics Lab., Wright Patterson Air Force Base, OH, AFFDL TR-70-126, July 1971.

[4]Freyman, R., "Actively Damped Landing Gear System," *Landing Gear Design Loads Conference*, CP-484, AGARD, No. 20, 1991, pp. 20.1–20.19.

[5]Ross, I., and Edson, R., "An Electronic Control for an Electro-Hydraulic Active Control Landing Gear for the F-4 Aircraft," NASA CR 3552, April 1982.

[6]Ross, I., and Edson, R., "Application of Active Control Landing Gear Technology to the A-10 Aircraft," NASA CR 166104, June 1983.

[7]Mc Gehee, J. R., and Carden, H. D., "A Mathematical Model of an Active Control Landing Gear for Load Control During Impact and Roll-Out," NASA TN D-8080, 1976.

[8]Howell, W. E., Mc Gehee, J. R., Daugherty, R. H., and Vogler, W. A., "F-106B Airplane Active Control Landing Gear Drop Test Performance," *Landing Gear Design Loads Conference*, CP-484, AGARD, No. 21, 1991, pp. 19.1–19.8.

[9]Mc Gehee, J. R., and Morris, D. L., "Active Control Landing Gear for Ground Load Alleviation," CP-384, AGARD, No. 18, 1985, pp. 1–12.

[10]Sutton, H. B., "The Potential for Active Suspension Systems," *Automotive Engineer*, London, Vol. 4, No. 2, 1979, pp. 21–24.

[11]Karnopp, D., "Active Damping in Road Vehicle Suspension System," *Vehicle Systems Dynamics*, Vol. 12, No. 6, 1983, pp. 291–316.

[12]Goodall, R. M., "Active Controls in Ground Transportation—a Review of the State-of-the-Art and Future Potential," *Vehicle Systems Dynamics*, Vol. 12, No. 4–5, 1983, pp. 225–257.

[13]Hedrick, J. K., "The Application of Active and Passive Suspension Techniques to Improve Vehicle Performance," Final Rept., U.S. Dept. of

Transportation, Contract DTRS5680-C-00018, March 1983.

[14]Vu K. T., "Advances in Optimal Active Control Techniques for Aerospace Systems; Application to Aircraft Active Landing Gear," N90-21769, Univ. of California, Los Angeles, 1989.

[15]Ghiringhelli, G. L., and Puccinelli, L., "The 'Passive' Approach to the Landing Gear Active Control," *Associazione Italiana Di Aeronautica e Astronautica National Congress Proceedings*, 1993, pp. 1731–1742.

[16]Ghiringhelli, G. L., Giavotto, V., Mantegazza, P., Boschetto, M., Casazza, A., and La Perna, G., "Ground and Manouvre Load Prediction of a Flexible Aircraft," *L'Aerotecnica—Missili e Spazio*, Vol. 65, No. 1/2, 1986, pp. 26–35.

[17]Ghiringhelli, G. L., and Boschetto, M., "Design Landing Load Evaluation by Dynamic Simulation of Flexible Aircraft," *Landing Gear Design Loads Conference*, CP-484, AGARD, No. 16, 1991, pp. 16.1–16.22.

[18]Fiume, I., and Ghiringhelli, G. L., "Combined Fuzzy-Deterministic Semi-Active Control of a Landing Gear," *Journal of Structural Control*, Vol. 2, No. 2, 1995, pp. 31–58.

[19]Bazzocchi, E., "Metodo di calcolo degli ammortizzatori oleopneumatici e confronti con i risultati ottenuti dalle prove," *L'Aerotecnica*, Vol. 35, No. 3, 1955, pp. 111–124.

[20]Moreland, W. J., "The Theory of Shimmy," *Journal of Aeronautical Sciences*, Vol. 21, No. 12, 1954, pp. 793–808.

[21]Smiley, R. F., "Correlation, Evaluation and Extension of Linearized Theories for Tire Motion and Wheel Shimmy," NACA TN-3632, June 1956.

[22]Djordjevich, A., "Modelling of Ground Effect on Aircraft," *Aerospace Simulation III, Proceedings of the SCS Multiconference*, San Diego, CA, Feb. 1988 (A89-19551 06-01), pp. 102–116.

[23]Pacejka, H. B., and Bakker, E., "The Magic Formula Tire Model," 1st Colloquium on Tyre Models for Vehicle Dynamics Analysis, *Vehicle System Dynamics*, Vol. 21, Supplement, pp. 1–18.

[24]Bakker, E., Pacejka, H. B., and Linder, L., "New Tire Model with an Application in Vehicle Dynamic Studies," *Progress in Technology*, SAE Int., Vol. 57, 1995, pp. 439–452.

[25]"ADAMS Tire," Ver. 9.2, Mechanical Dynamics, Inc., Rel. 8.0, Ann Arbor, MI, Nov. 1994.

[26]"DADS User's Manual: Tire Force," Ver. 7.5, Computer-Aided Design Software, Inc., Rel. 8.0, Coralville, Nov. 1995.